Ability of NCAR RegCM2 in Reproducing the Dominant Physical Processes during the Anomalous Rainfall Episodes in the Summer of 1991 over the Yangtze–Huaihe Valley①

Luo Yong (罗 勇)②, Zhao Zongci (赵宗慈) and Ding Yihui (丁一汇)

National Climate Center, Beijing 100081

(Received March 21, 2001; revised December 10, 2001)

ABSTRACT

The excessively torrential rainfall over the Yangtze–Huaihe valley during the summer of 1991 is simulated with an updated version of the second generation NCAR regional climate model (RegCM2) as a case study to evaluate the model's performance in reproducing the daily precipitation and the associated physical factors contributing to the generation of the anomalous rainfall. This simulation is driven by large–scale atmospheric lateral boundary conditions derived from the European Center for Medium Range Weather Forecast (ECMWF) analysis. The simulation period is May to August 1991. The model domain covers East Asia and its adjacent oceanic regions. The model resolution is 60 km × 60 km in the horizontal and 23 layers in the vertical.

The model can reasonably reproduce the daily precipitation events over East Asia for the summer of 1991, especially in the Yangtze–Huaihe valley where the anomalous rainfall occurred. The spatial and temporal structure of some important physical variables and processes related to the generation of the anomalous rainfall are analyzed. The time evolution of simulated upward vertical motion and horizontal convergence agrees with the five rainfall episodes over this subregion. The water vapor feeding the rainfall is mostly transported by the horizontal atmospheric motions from outside of the region rather than from local sources. The subtropical high over the western Pacific Ocean controls the progress and retreat of the summer monsoon over East Asia, and the RegCM2 can simulate the northward migration and southward retreat of subtropical high over the western Pacific Ocean. Furthermore, the model can represent the daily variation of the low level jet, which is crucial in the water vapor transport to the Yangtze–Huaihe valley.

Key words: Regional climate modeling, Daily rainfall, The Yangtze–Huaihe valley

1. Introduction

In recent years, regional climate models have been widely used for high resolution simulation and study of regional climate anomalies. In particular, the regional climate model

---

①*Corresponding author address:* Dr. Luo Yong, National Climate Center, China Meteorological Administration, Beijing, 100081.

This research was jointly supported by National Key Programme for Developing Basic Sciences (G1998040900 Part 1), the USA / DOE–PRC / CMA Joint Research on Regional Climate, the National Key Project of Studies on Short–Range Climate Prediction System in China under Grant 96–908–02–04.

②E–mail: yluo@cma.gov.cn

(RegCM) developed at National Center for Atmospheric Research (NCAR) has been widely used by the scientific community for simulating regional climate over a range of areas, such as the United States, Sahel, Europe–East Atlantic and East Asia–Pacific (Zhao and Luo 1997). In particular, Gong et al. (1996), Zhang (1996), Liu et al. (1996), Luo and Zhao (1997), Fu et al. (1998), Wei et al. (1998), Wei and Wang (1998) used NCAR RegCM or other regional climate models to evaluate the model ability in simulating the summer climate of East Asia. One common feature of most experiments was a relatively low vertical resolution, which varied between 10 and 14 levels. At the current stage, the global climate models such as NCAR CCM which is usually coupled with RegCM have 18 vertical layers. Thus, the regional climate model which aims to model the detail of regional climate change should have the vertical resolution not lower than that of global climate models. In addition, previous studies did not analyze the physical variables or processes related to the formation of the East Asian climate anomalies. In fact, the RegCM provides some diagnostic variables and physical processes, such as surface latent and sensible heat fluxes, turbulent heating and moistening, which are not available from operational observations and can be used for a better understanding of the genesis and maintenance of the East Asian climate anomalies. Furthermore, these studies mostly focused on monthly and seasonally averaged precipitation and surface air temperature and did not examine in depth the model performance at shorter time scales. Indeed, synoptic and mesoscale systems developing at daily to weekly time scales, such as fronts, low–level jets and vortices have a direct influence on summer precipitation over East Asia. The distribution of summer precipitation over East Asia is extremely non–uniform, both spatially and temporally (Ding 1991). Finally, the regional climate model will be coupled with hydrological model and agriculture model. This requires evaluating the ability of regional climate model in reproducing daily rainfall and other meteorological variables over East Asia.

In the summer of 1991 (mainly in the period from May to July) severe rainfall events and flooding occurred in the Yangtze–Huaihe valley, which is located in East China. This anomalously heavy rainfall had characteristics of long persistence, large amount of precipitation and large extent of affected areas rarely seen in this century (Ding 1993). This extreme event is an appropriate case to be selected to highlight the model performance of RegCM. In this paper, an updated version of the NCAR RegCM2 was used in the numerical simulation of the East Asia summer monsoon season of 1991. Luo and Zhao (1997) and Leung et al. (1999) examined the monthly and seasonally mean aspects of model performance to evaluate the ability of RegCM2 in simulating the general characteristics of the anomalous East Asia summer monsoon in 1991. The focus of this paper is on the model performance in simulating daily precipitation and on the associated physical processes that contributed to this severe rainfall event. Section 2 first describes model and experiment design for this study. Section 3 is devoted to evaluate the ability of the RegCM2 in reproducing the daily precipitation over the Yangtze–Huaihe valley, and section 4 is dedicated to analyze if the model has the ability in reproducing the spatial and temporal structure of some important physical variables and processes associated to the formation of the torrential rainfall. The effects of large–scale circulations on the generation and maintenance of the rainfall is presented in section 5, and the main conclusions of the study are given in section 6.

2. Brief introduction of NCAR RegCM2 and experiment design

RegCM2 is a second–generation regional climate model developed at NCAR. Its dynamical component is essentially the same as that of the NCAR / PSU MM4 (Anthes et al. 1987), which is a *primitive equation and grid point model*, while physics parameterizations include the Biosphere–Atmosphere Transfer Scheme (BATS, Dickinson et al. 1992), an explicit planetary boundary layer scheme (Holtslag et al. 1990), the radiative transfer package of the NCAR CCM2 (Briegleb 1992), and an updated Arakawa–type convective scheme (Grell 1993). Furthermore, RegCM2 has an option for coupling with an interactive lake model (Hostetler and Giorgi 1992). A detailed description of the model is given by Giorgi et al. (1993a, b).

Since 1993, the NCAR RegCM2 has been modified in some aspects, with primary modification including the incorporation of an updated version of the Grell convective scheme, a simplified explicit moisture scheme, the adaptation of the saturation vapor pressure formula from MM5, modified computation of the pressure gradient term, modifications to BATS and lake model, optimized computation of the PBL scheme, and several parameter adjustments. A recent version of the model has been used for this study, and a series of preliminary experiments have completed to optimize the model prior to this study.

The model is integrated for a period from May 1 to August 31, 1991, for a total of 123 days. The atmospheric temperature, water vapor mixing ratio, pressure and wind fields in the initial and lateral boundary conditions are derived from ECMWF analyses of observations at a resolution of T42 truncation in horizontal and 15 layers in vertical (Trenberth and Olson 1988). *The lateral boundary conditions are updated every 12 hours, and observed monthly* mean SST are from Shea et al. (1992). The soil temperature is initialized by the observed data at 0000Z May 1st, 1991 provided by ECMWF. Soil water content is initialized as described in Giorgi and Bates (1989), i.e., the initial soil water content depends on the type of vegetation.

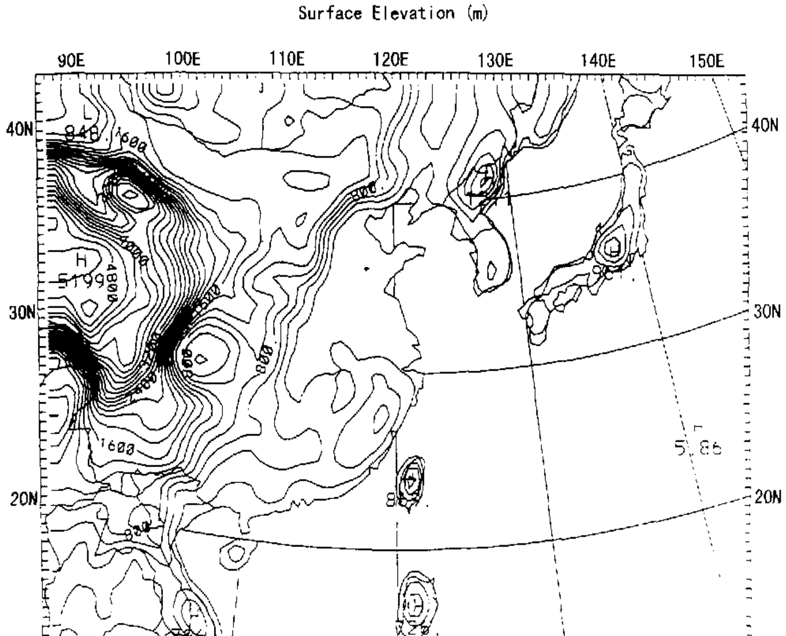

Fig. 1. The model domain and topography. Contour interval is 200 m.

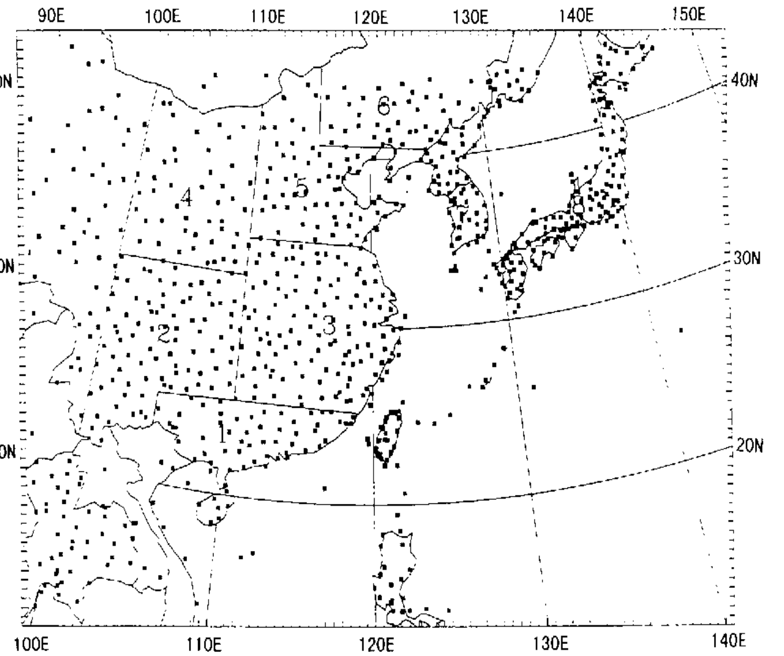

Fig. 2. The location of observation stations and regionalization. 1–South China, 2–Southwest China, 3–the Yangtze–Huaihe valley, 4–Northwest China, 5–North China, 6–Northeast China, 7–Korea and 8–Japan.

The model vertical resolution for our experiments is 23 layers with the model top at 10 hPa. There are 4 layers with sigma value less than 0.2, 7 layers greater than 0.8, and 12 layers equally spaced. The model domain is shown in Fig. 1. It covers East Asia and the western Pacific. It is about 3840 km × 5040 km in size with a grid spacing of 60 km, and center at 30°N and 120°E. An 18–layer buffer zone is applied in this study with an exponential relaxation technique which can provide smooth transition from large–scale driving fields to the internal high–resolution information produced by the model.

The daily precipitation simulated by RegCM2 is validated against observation data archived at NCAR from the U.S. National Meteorological Center (NMC). The documentation of this data is available from the NCAR Data Analysis Division. Fig. 2 presents the location of the observation stations. The distribution of stations is rather dense and homogeneous and a total of 848 stations are found within the model domain. The simulated precipitation at model grid points is interpolated onto the location of each station by bilinear interpolation and then compared with the observations. Eight subregions are also selected for more detailed analysis, i.e., South China, Southwest China, the Yangtze–Huaihe valley, Northwest China, North China, Northeast China, Korea and Japan (see Fig. 2). Table 1 shows the number of stations located in each subregion. The same ECMWF large–scale analysis datasets used for the initial and lateral boundary conditions is employed for validation of the simulated atmospheric variables.

Table 1. The station numbers in each subregion

Subregion No.	Subregion Name	Station Number
1	South China	108
2	Southwest China	84
3	The Yangtze–Huaihe valley	128
4	Northwest China	50
5	North China	72
6	Northeast China	41
7	Korea	58
8	Japan	156

3. Simulation of daily precipitation over the Yangtze–Huaihe valley

In this section, we evaluate the ability of RegCM2 in reproducing daily precipitation, especially over the Yangtze–Huaihe valley, i.e., subregion 3 of Fig. 2 where the flood events occurred in the summer of 1991.

The observations and simulation of daily precipitation over subregion 3 (the Yangtze–Huaihe valley) during May–August 1991 is shown in Fig. 3. The correlation coefficient between the observations and simulation is 0.55, which is in the middle of the range of correlation coefficients calculated for the various regions (see Table 2). In the summer of 1991, there were five rainfall episodes over this area, i.e., May 3–7 (day 3–7), May 18–26 (day 18–26), June 2–19 (day 33–50), June 30–July 13 (day 61–74) and July 28–August 11 (day 89–103), among which the middle three episodes were defined as Meiyu (Ding, 1993). Compared with the observations, RegCM2 can not only reproduce the time of occurrence, but also the intensity of the rainfall episodes, except for an overestimation of rainfall around May 11 and during July 12–23.

Table 2. The average and standard deviation of regional averaged daily precipitation and the correlation coefficient between simulation and observation during May–August 1991 over East Asia

Subregion	Average (mm d^{-1})		Standard Deviation (mm d^{-1})		Correlation
	Observation	Simulation	Observation	Simulation	
1	5.08	8.64	5.60	7.20	0.70
2	4.45	3.27	2.79	2.43	0.38
3	4.04	4.83	3.53	3.57	0.55
4	1.39	1.82	1.95	2.46	0.61
5	2.47	2.62	3.54	3.34	0.64
6	2.75	2.18	4.40	3.04	0.74
7	5.44	4.79	7.73	6.38	0.55
8	4.81	6.52	4.50	6.49	0.49

Table 2 presents the average and standard deviation of subregional averaged daily precipitation and the correlation coefficient between simulation and observation during May–August 1991 over East Asia. Among the eight subregions, the simulation of daily precipitation in subregion 6 (Northeast China) is the best in which the correlation coefficient is as high as 0.74. The order of subregions according to the correlation coefficients from the

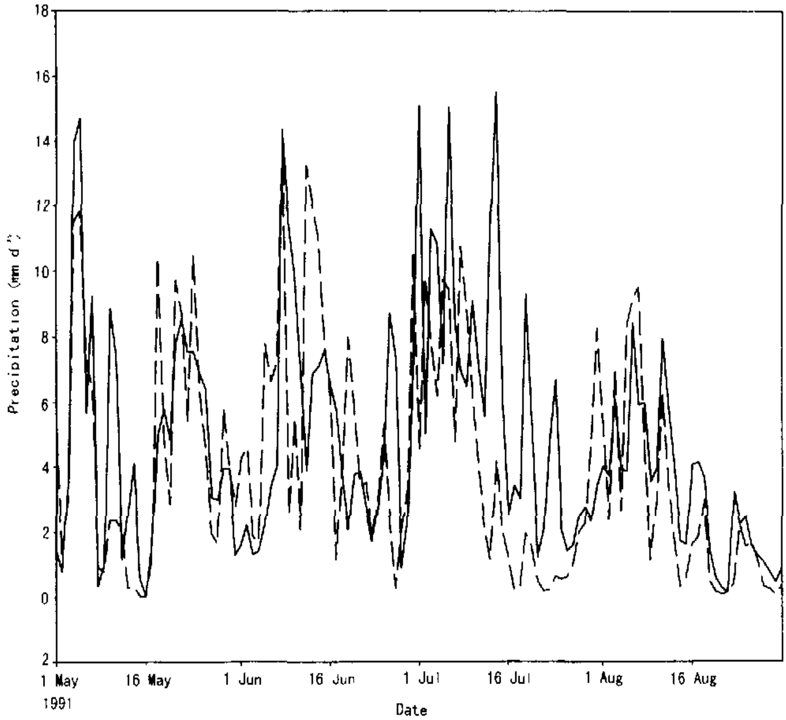

Fig. 3. The simulation (solid line) and observation (dashed line) of daily precipitation in mm d^{-1} over subregion 3 (the Yangtze–Huaihe valley) during May–August 1991. The correlation coefficient between the observation and simulation is 0.55.

highest to the lowest is subregions 6, 1 (South China, 0.70), 5 (North China, 0.64), 4 (Northwest China, 0.61), 3 (the Yangtze–Huaihe valley, 0.55), 7 (Korea, 0.55), 8 (Japan, 0.49) and 2 (Southwest China, 0.38). Though the ability of RegCM2 in reproducing daily precipitation varies among the subregions, all the correlation coefficients are above that of the significance level of 0.01, i.e., 0.244, which, given that the complex physiography of East Asia is likely reflected at individual station location and that the model is run at a relatively coarse resolution, are an indication of a reasonably good performance. Thus, we can conclude that RegCM2 is capable of simulating the daily precipitation in the summer 1991 over East Asia.

From Table 2 it can be seen that for most subregions, if the average of simulated daily precipitation is greater (less) than that of the observations, the standard deviation of simulation is also greater (less) than that of the observations. This suggests that there is a close relation between the average and day–to–day variability of subregional mean daily precipitation. If the day–to–day variability of simulated rainfall is too large (small), there are be more (less) days with larger simulated rainfall than observed so as to make the average of simulated precipitation larger (less) during May–August 1991.

RegCM2 can simulate well the spatial distribution of the standard deviation of daily precipitation, i.e., the subregion to subregion difference. For example, both in the model and in the observations the three subregions with the largest standard deviation of daily precipitation are subregions 7 (Korea), 1 (South China) and 8 (Japan) and the two subregions with the lowest standard deviation of daily precipitation are subregions 2 (Southwest China) and 4 (Northwest China).

4. Spatial and temporal structure of rainfall

This section is dedicated to analyze the spatial and temporal structure of some important physical variables and processes associated to the rainfall formation, including vertical velocity and horizontal divergence, surface sensible and latent heat fluxes, and atmospheric heat source and vapor sink.

4.1 *Vertical velocity and horizontal divergence*

To analyze the features of atmospheric motion over the Yangtze–Huaihe valley in the summer of 1991, we show in Fig. 4 the time–height section of simulated and analyzed vertical velocity averaged over the subregion 3 (the Yangtze–Huaihe valley). Both in the model and analysis, upward atmospheric motion (negative values) is found in correspondence with the five rainfall episodes over this subregion. In the model simulation, among these three Meiyu episodes, the upward motion of the third stage of Meiyu (June 30–July 13) is the most intense, with a maximum center of approximately −0.003 hPa s^{-1} at 550 hPa. Intercomparison among the three stages of Meiyu indicates that the later the stage, the more intense the upward motion. Figure 4a also shows that the five periods with upward motion are separated by periods with predominant downward atmospheric motion. The large scale analysis also shows the largest upward motion occurred at the third stage of Meiyu, but at a little bit higher height (Fig. 4b). Due to the relatively coarse resolution, analysis cannot present the downward atmospheric motions among the three Meiyu rainfall episodes as in the model simulation. The regional climate model has the advance in reproducing the details of atmospheric structure in correspondence with Meiyu rainfall.

The time–height section of simulated and analyzed horizontal divergence averaged over subregion 3 (the Yangtze–Huaihe valley) is shown in Fig. 5. We can see that in both of the model and analysis, lower level convergence and upper level divergence dominate throughout the integration period. The level of non–divergence is located at approximately 400–500 hPa. Five centers of maximum low level convergence and upper level corresponding divergence are found in correspondence with the five rainfall episodes. Especially in the model simulation (Fig. 5a), at the first stage of Meiyu (May 18–26), the convergence was shallow, limited to levels below 700 hPa. At the second stage (June 2–19), the convergence level reached 500 hPa and at the third stage (June 30–July 13) the convergence level reached as high as 350 hPa. But in the large scale analysis (Fig. 5b), the day–to–day variation of horizontal divergence is smoother and the change in height of convergence level among the three Meiyu rainfall episodes cannot be found.

Figures 4 and 5 illustrate a dynamical process by which, during the five rainfall episodes, water vapor is transported horizontally into the Yangtze–Huaihe valley by convergence at the lower levels, transported upward to the upper levels by vertical motion and out of the region by divergenec at upper levels. The model simulation is quite consistent with large scale analysis but can reproduce clearly the details of atmospheric structures.

4.2 *Surface sensible and latent heat fluxes*

Figure 6 presents the simulated daily–averaged surface sensible heat flux over the Yangtze–Huaihe valley during May–August 1991. Comparison with Fig. 3 clearly indicates

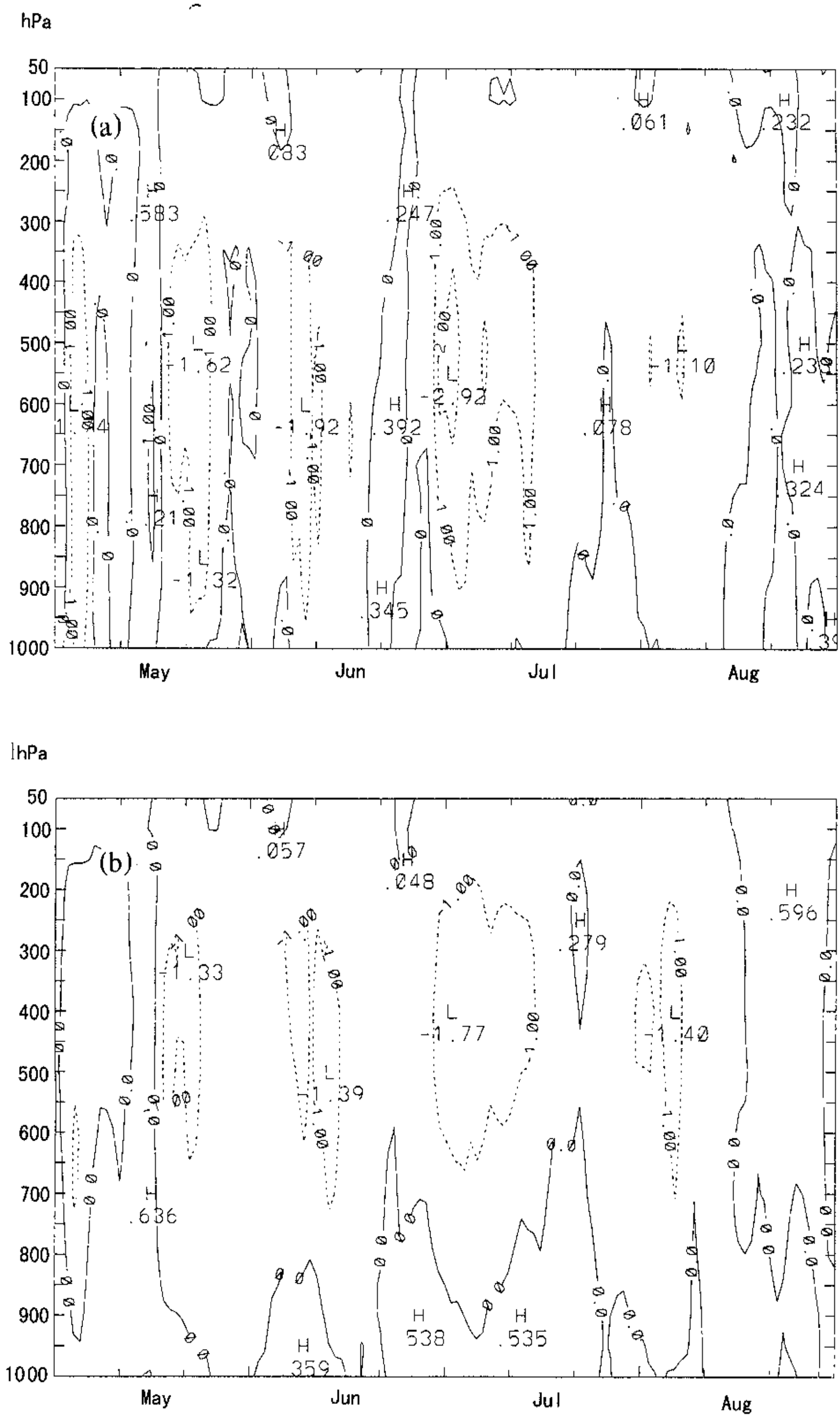

Fig. 4. Time–height section of simulated (a) and analyzed (b) vertical velocity averaged over subregion 3 (the Yangtze–Huaihe valley) in 10^{-3} hPa s^{-1}. Contour intervals are 1×10^{-3} hPa s^{-1}. A 3–day moving average has been applied.

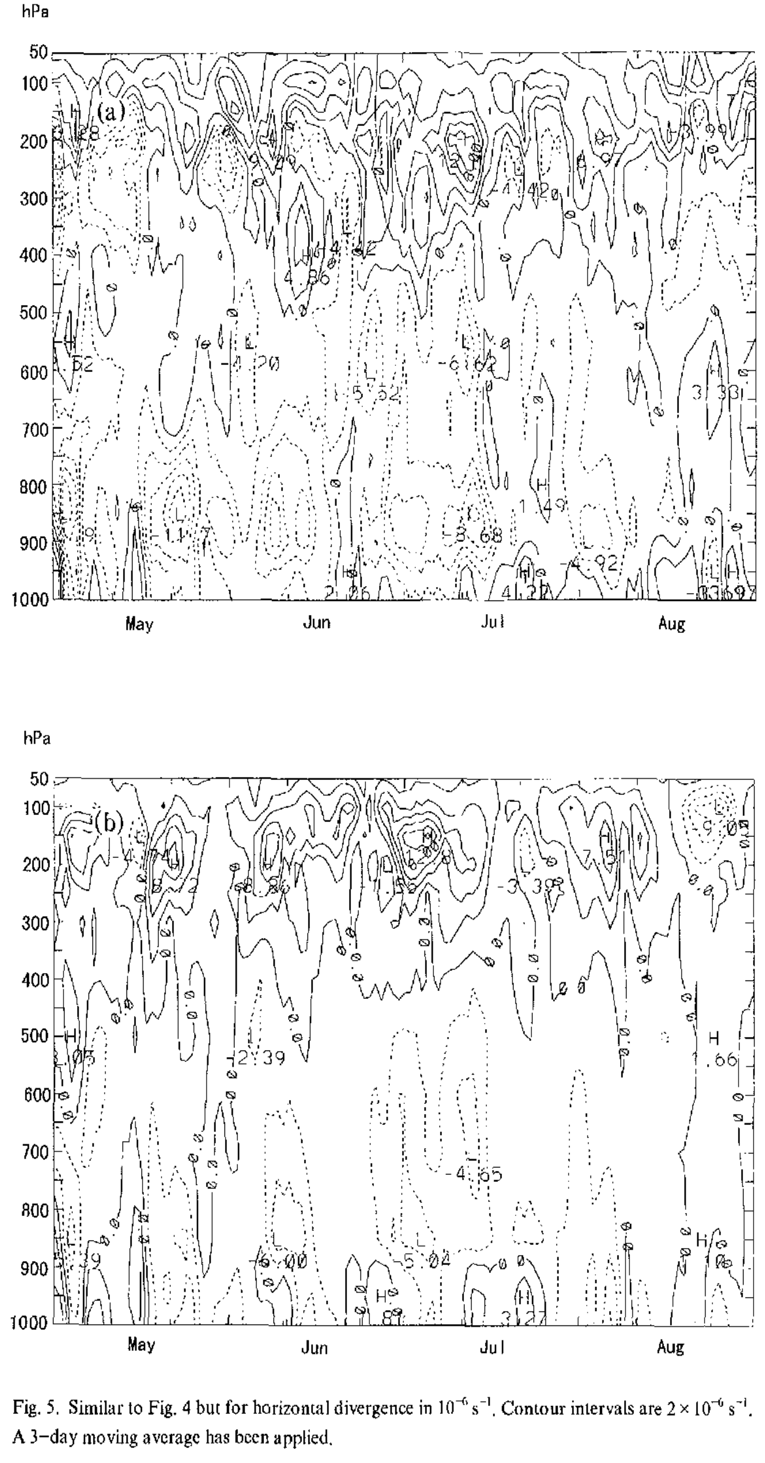

Fig. 5. Similar to Fig. 4 but for horizontal divergence in $10^{-6}\ s^{-1}$. Contour intervals are $2\times10^{-6}\ s^{-1}$. A 3-day moving average has been applied.

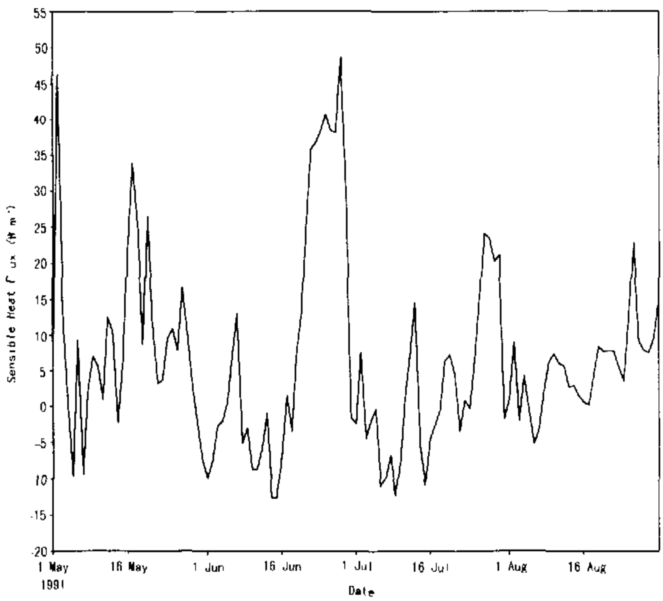

Fig. 6. The simulated daily surface sensible heat flux in W m^{-2} over subregion 3 (the Yangtze–Huaihe valley) during May–August 1991.

that during the rainfall episodes the surface sensible heat flux is lower than that during the break periods, except for the first stage of Meiyu, when the precipitation is dominant of convective nature and the total cloudiness is lower compared with the other three rainfall episodes (not shown) so that more solar radiation heats the surface. In general the average of sensible heat flux over all rainfall periods is 3.16 W m^{-2}, while during the breaks between rainfall episodes the average is as large as 12.26 W m^{-2}, i.e. almost 4 times the average during rainfall periods.

The simulated daily surface latent heat flux over the same subregion during May–August 1991 is shown in Fig. 7. There is lower latent heat flux during the rainfall periods, i.e., 45.42 W m^{-2} on an average, than during break periods, i.e., 57.52 W m^{-2} on an average. The relatively lower latent heat flux during rainfall periods suggests that the water vapor to feed the heavy rainfall is mostly transported by horizontal atmospheric motions from outside of the region rather than produced locally. The differences in latent and sensible heat fluxes during rainfall and break periods can be explained in terms of greater energy input to the surface by insolation due to lower cloudiness in the break periods (not shown). The surface solar radiation is in turn partitioned in energy for latent and sensible heat fluxes. Our results agree with the conclusions achieved by the diagnostic analysis with observation station data by Wu et al. (1996).

4.3 *Vertical structure of heat source and vapor sink*

To further understand the thermodynamic structure of the torrential rainfall over the Yangtze–Huaihe valley, we can analyze the time–height section of simulated heating and moistening produced by convection, large–scale condensation and turbulence transport.

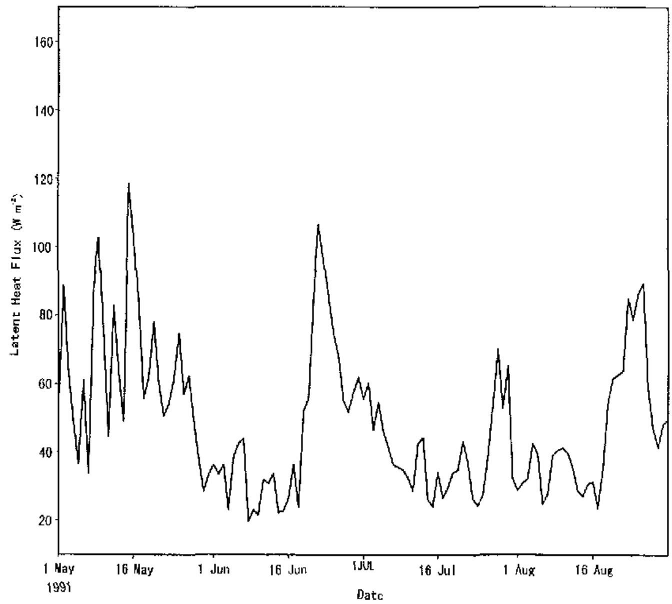

Fig. 7. Similar to Fig. 6 but for latent heat flux.

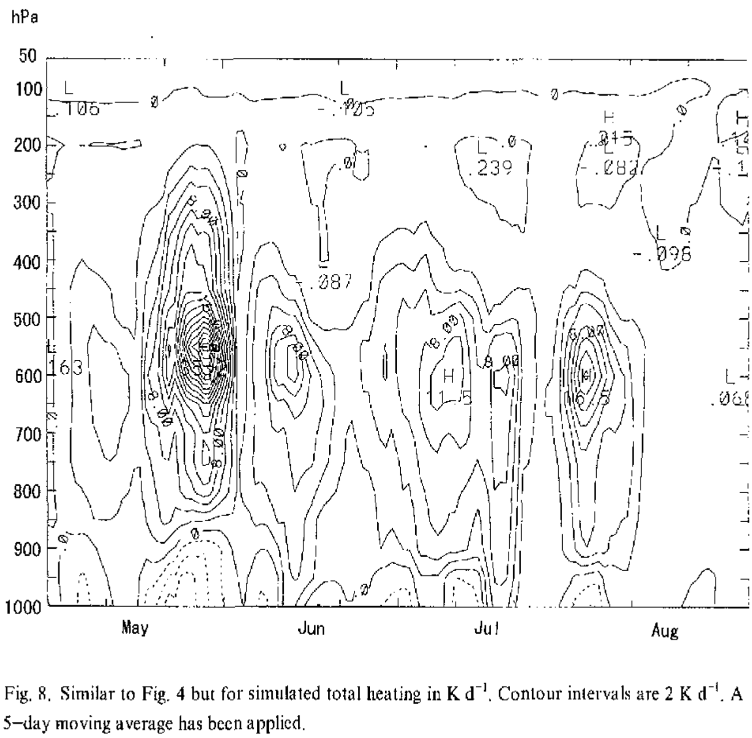

Fig. 8. Similar to Fig. 4 but for simulated total heating in K d^{-1}. Contour intervals are 2 K d^{-1}. A 5–day moving average has been applied.

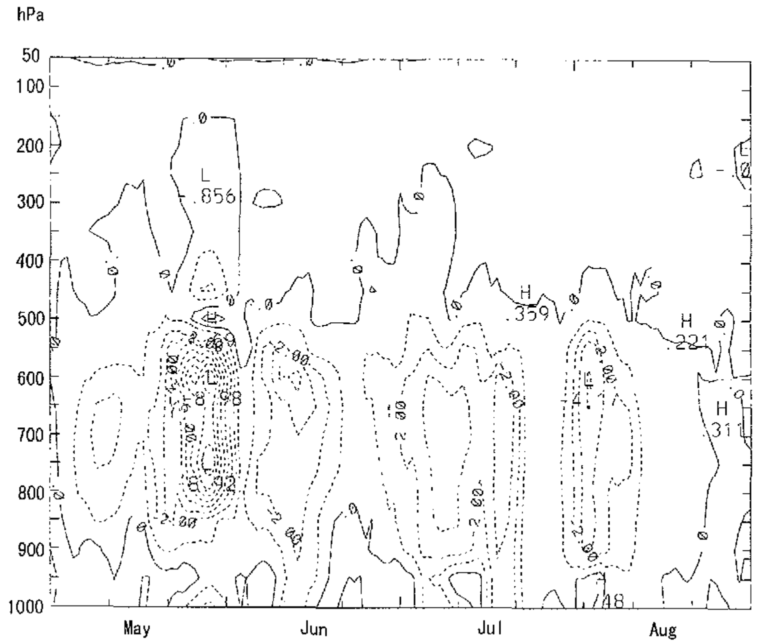

Fig. 9. Similar to Fig. 4 but for simulated total moistening in g kg^{-1} d^{-1}. Contour intervals are 1 g kg^{-1} d^{-1}. A 5–day moving average has been applied.

averaged over this subregion, shown in Figs. 8 and 9, respectively. Except in the lower boundary layer and upper atmosphere, heating and drying dominate in the troposphere throughout the simulation period. Five heating and drying maximum centers can be identified in correspondence with the five rainfall episodes. All the maxima in heating and drying occur below 500 hPa, because of the higher water vapor content in the middle and lower troposphere, and among the five rainfall episodes, the heating and drying are the largest in the first stage of Meiyu, when the precipitation is mainly produced by convection.

5. Large–scale circulations

5.1 *Subtropical high over the western Pacific Ocean*

The subtropical high over the western Pacific Ocean is the most important planetary scale system which controls the progress and retreat of the summer monsoon over East Asia. In order to evaluate the ability of RegCM2 in simulating the time evolution of the western Pacific subtropical high, which directly contributes to the production of rainfall over the Yangtze–Huaihe valley, Figs. 10a and 10b show a time–latitude section of the analyzed and simulated 500 hPa geopotential height along 130°E meridian during the integration period. A 5–day moving average is applied. The extension of the subtropical high is roughly defined by the geopotential heights greater than 5880 m.

From the analyzed data shown in Fig. 10a, we can see that during the integration period, there were three stages of the northward progress of subtropical high over the western Pacific

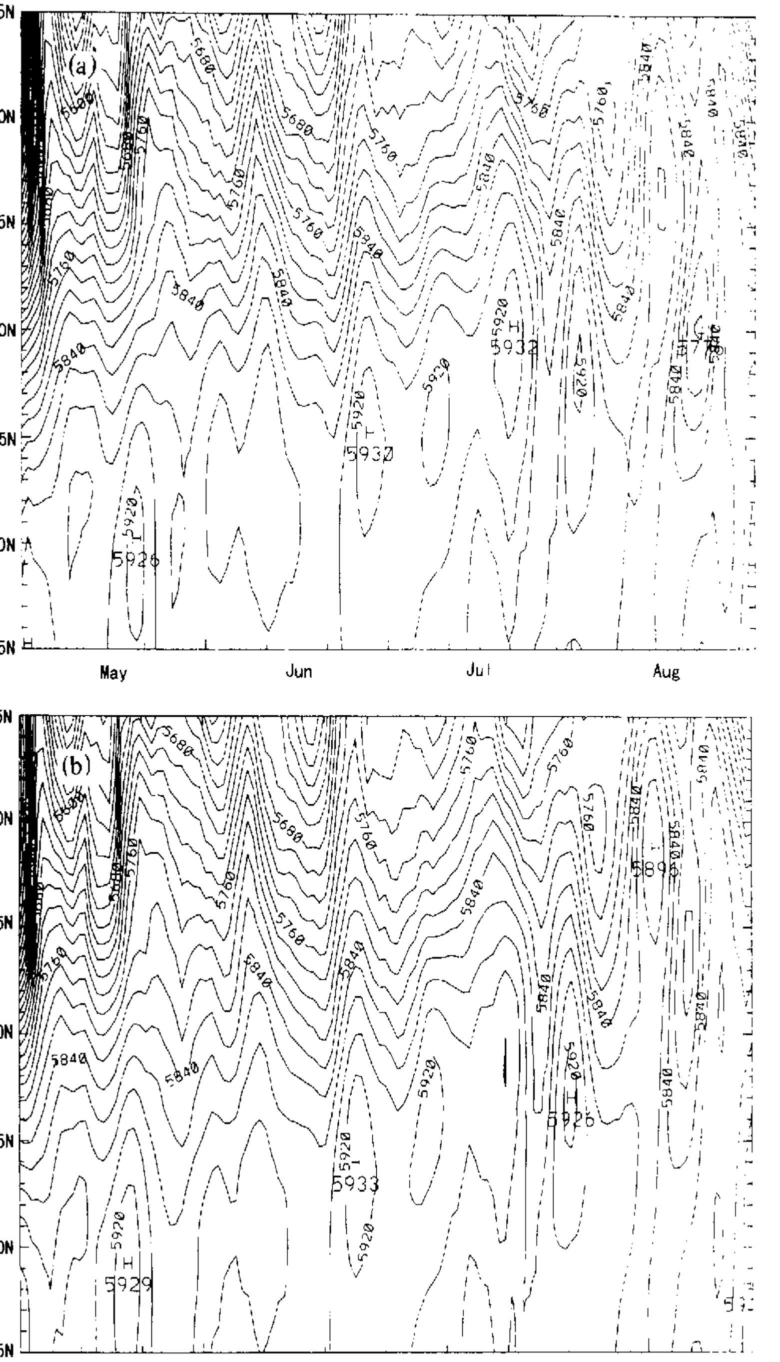

Fig. 10. Time-latitude sections of 500 hPa geopotential height along the 130°E meridian for ECMWF analysis (a), and RegCM2 simulation (b). Contour intervals are 20 m. A 5-day moving average has been applied.

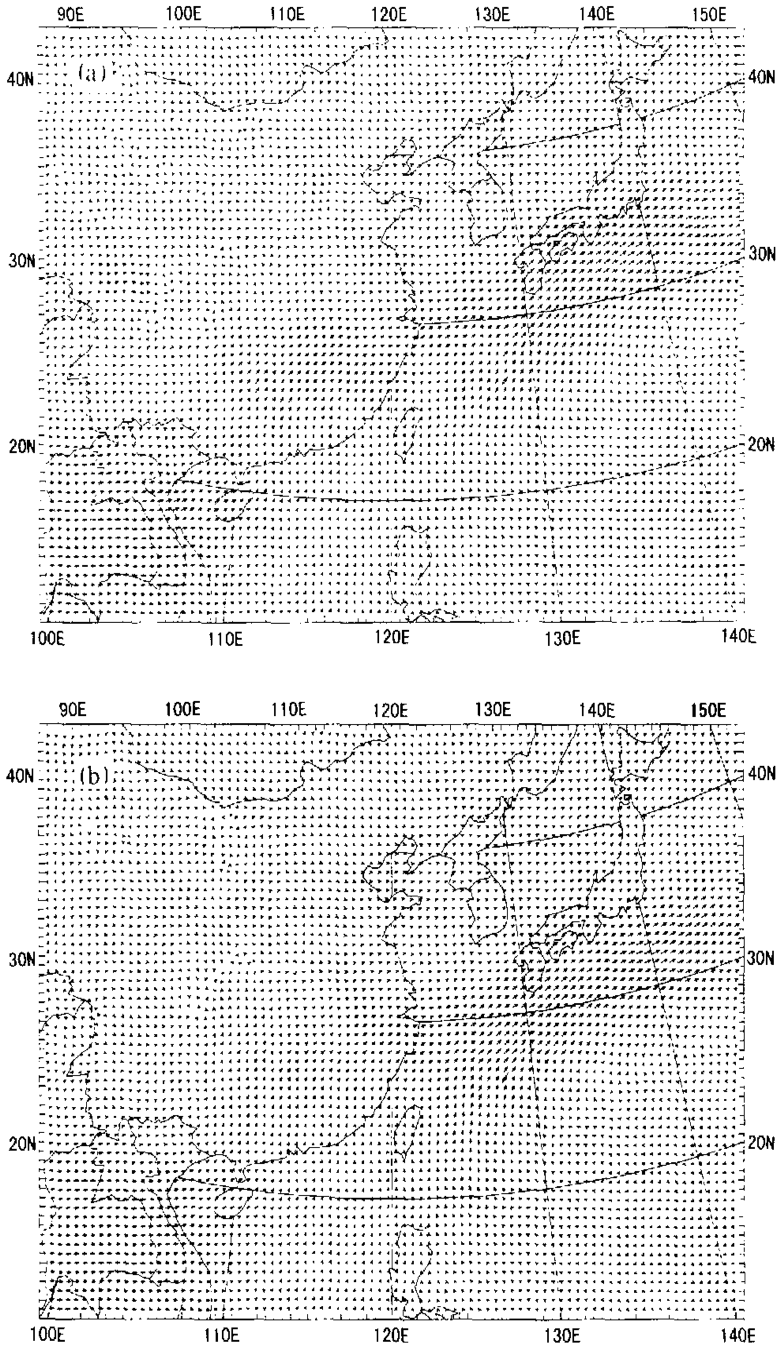

Fig. 11. Simulated (a) and analyzed (b) mean 850 hPa wind in m s^{-1} in June 1991. Maximum vector is 12.2 m s^{-1} for (a) and 11.9 m s^{-1} for (b)

Ocean. The first stage occurred in May when the subtropical high jumped from 22°N to 26°N and remained around 24°N to 27°N. This indicates the start of the rainy season over the Yangtze–Huaihe valley. The second stage began in the end of May when the subtropical high jumped from 23°N to 29.5°N and remained around 28°N to near 32°N. This stage of movement of the subtropical high corresponded to the second stage of Meiyu. When the subtropical high jumped from 25°N to 32°N in the last ten days in June, the third stage of Meiyu began, during which the subtropical high fluctuated from 29°N to 37°N. When the subtropical high migrated north of 33°N in the middle of July, the Meiyu episode ended. Between the three stages of subtropical high northward movement, the high retreated southward to generate the breaks in Meiyu episodes.

Compared with the analysis, RegCM2 simulated well the northward migration and southward retreat of the subtropical high over the western Pacific Ocean (Fig. 10b) except during the third stage when the subtropical high jumped northward to 37°N around July 20. In the RegCM2 simulation, the subtropical high did not jump as far north as in the analysis, and it only reached 35°N. This is the main reason why RegCM2 overestimated precipitation between July 14 and 25 (Fig. 3).

5.2 *Low level jet and water vapor transport*

The analysis in subsection 4.2 indicates that the water vapor that fed the torrential rainfall over the Yangtze–Huaihe valley was not mostly produced locally by evaporation but was transported over the region by large scale circulations. Previous studies revealed that the low level jet in summer over East China plays an important role in the water vapor transport (Ding 1993). To evaluate the ability of RegCM2 in simulating the low level jet and its effect on water vapor transport, here we present the simulation and analysis of averaged 850 hPa wind (Fig. 11) and 700 hPa relative humidity (Fig. 12) in June 1991. In the 850 hPa wind field, it can be clearly noted that there exists a strong low level jet extending from the Indo–China Peninsula to South China and from there to the Yangtze–Huaihe valley. A high relative humidity tongue at 700 hPa is associated with the low level jet. It can be deduced that in the model simulation the water vapor available to generate the torrential rainfall is indeed transported to the Yangtze–Huaihe valley by a southwesterly low level jet, say from the Bay of Bengal. The model simulations are quite consistent with large scale analyses.

Figure 13 presents the daily evolution of 700 hPa v–component wind averaged over the Yangtze–Huaihe valley throughout the integration period for both the ECMWF analysis and RegCM2 simulation. It can be seen that during the five episodes of rainfall a strong northward wind ($v > 0$) prevailed. At other levels, i.e., 1000 hPa and 850 hPa, the v–component of the wind had similar characteristics of time evolution (not shown). Compared with the ECMWF analysis (dashed line), the RegCM2 simulates well this day–to–day variation of low level jet (solid line).

6. Summary and conclusions

This study evaluates the ability of NCAR RegCM2 in representing the torrential rainfall over the Yangtze–Huaihe valley in May–August 1991. Because this extremely heavy rainfall period was exceptional for its long persistent time, large amount of rainfall, extensive hitting areas and severity of damages, it provides an excellent case to investigate the model performance in simulating East Asian monsoon climate, especially at high temporal scales.

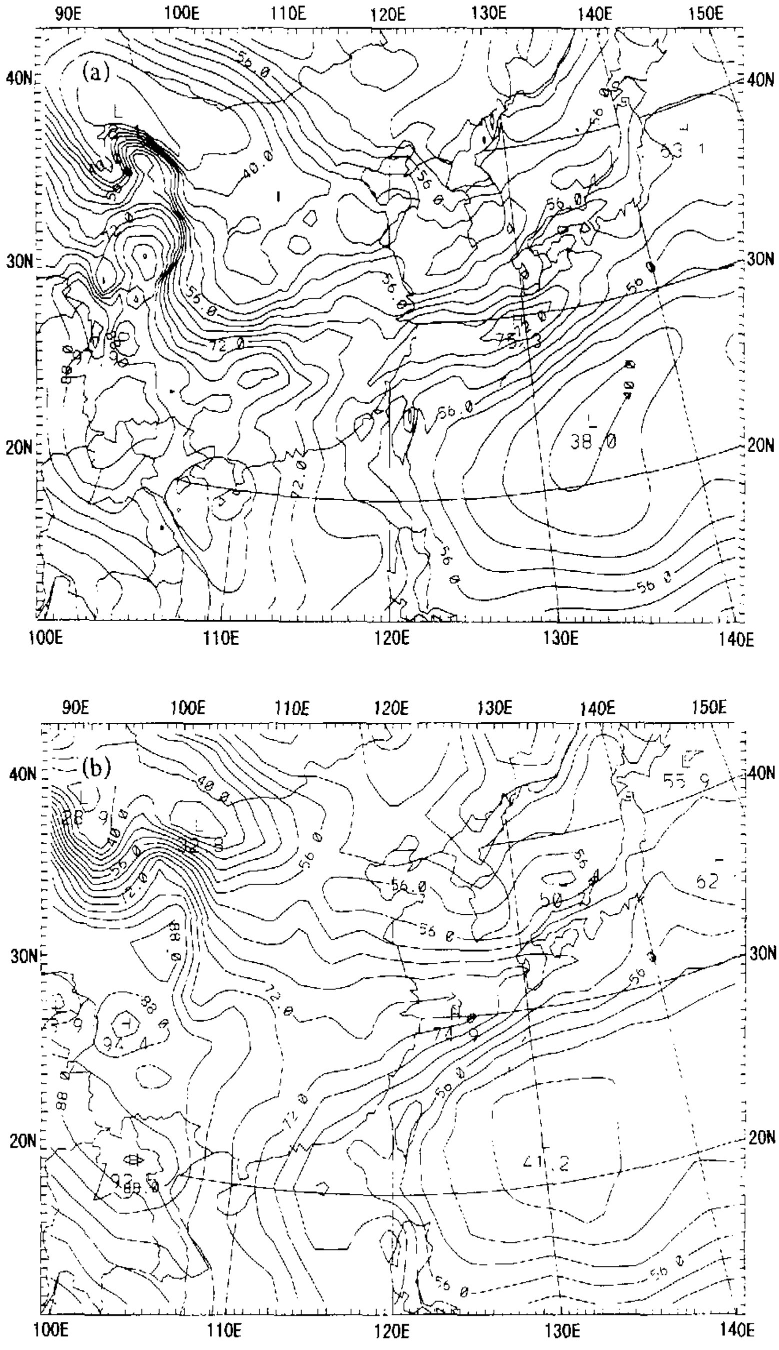

Fig. 12. Similar to Fig. 11 but for 700 hPa relative humidity (%). Contour interval is 4%.

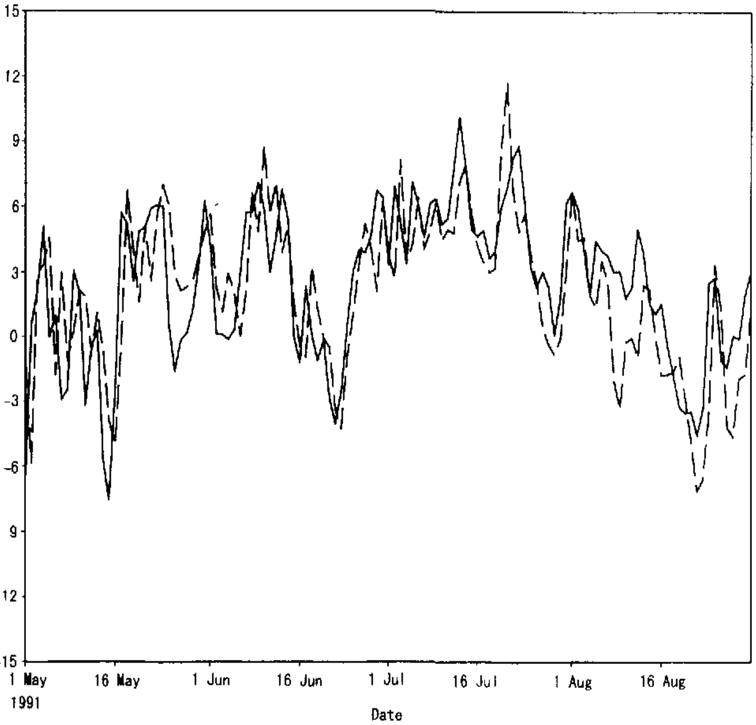

Fig. 13. Similar to Fig. 3 but for daily 850 hPa v–component wind in m s^{-1}.

The model reproduced reasonably well daily precipitation over East Asia for the simulation period, although this ability varied somewhat among the subregions. The correlation coefficients for all eight subregions were well above that of significance level of 0.01. Especially over the Yangtze–Huaihe valley, where the torrential rainfall occurred, RegCM2 reproduced not only the time of occurrence, but also the intensity of different rainfall episodes. Moreover, the model simulated well the spatial distribution of the standard deviation of daily precipitation.

The time evolution of simulated upward vertical motion and horizontal convergence agreed with the five rainfall episodes over this subregion. The relatively low latent heat flux during rainfall periods indicates that the water vapor necessary to maintain the rainfall was transported by the horizontal atmospheric motions from afar rather than produced locally. The water vapor is transported horizontally to the Yangtze–Huaihe valley by lower level convergence during the five rainfall episodes. Five heating and drying centers dominated during the five rainfall episodes. The model simulations are very consistent with large scale analyses and moreover can provide the detailed structure of atmospheric motions during the rainfall and break periods, which is one of the significant advances of regional models due to higher resolutions.

The subtropical high over the western Pacific Ocean is the most important planetary scale system which controls the progress and retreat of summer monsoon over East Asia.

RegCM2 can simulate well the northward migration and southward retreat of the subtropical high over the western Pacific Ocean. Furthermore, the model can represent the day-to-day variations of low level jet, which is very important in the water vapor transport to the Yangtze-Huaihe valley.

The authors wish to thank sincerely Dr. R. Leung and S. Ghan for their kind help and suggestions. The views expressed herein are those of the authors and do not necessarily reflect theirs. The data conditions they provided were essential to the completion of this paper. We also wish to thank Dr. F. Giorgi, G. Bates, C. Shields, Liu Yongqiang, Sun Liqiang, Song Yi, Shen Wenhai, Li Ji, Lu Er, W. -C. Wang and Wei Helin for providing the model code and helpful discussions.

REFERENCES

Anthes, R. A., E. -Y. Hsie, and Y. -H. Kuo, 1987: *Description of the Penn State / NCAR Mesoscale Model Version 4 (MM4)*. NCAR Tech. Note, NCAR / TN-282+STR, 66pp.

Briegleb, B. P., 1992: Delta-Eddington approximation for solar radiation in the NCAR Community Climate Model. *J. Geophys. Res.*, **97**, 7603-7612.

Dickinson, R. E., A. Henderson-Sellers, and P. J. Kennedy, 1992: Biosphere-Atmosphere Transfer Scheme (BATS) version 1E as coupled to the NCAR Community Climate Model. NCAR Tech. Note, NCAR / TN-387+STR, 72pp.

Ding Yihui, 1991: Summer monsoon rainfall in China. *J. Meteor. Soc. Japan*, **70**(1B) (Special Edition on Asian Monsoon), 243-266.

Ding Yihui, 1993: *Studies on the Excessively Storm Rainfall over the Yangtze-Huaihe Valley in 1991*. China Meteorological Press, Beijing, 255pp, (in Chinese).

Fu Congbin, Wei Helin, Chen Ming, Su Bingkai, Zhao Ming, and Zheng Weizhong, 1998: Simulation of the evolution of summer monsoon rainbelts over eastern China from regional climate model. *Scientia Atmospherica Sinica*, **22**(4), 522-534.

Giorgi, F., 1991: Sensitivity of simulated summertime precipitation over the western United States to different physics parameterizations. *Mon. Wea. Rev.*, **119**, 2870-2888.

Giorgi, F., Y. Huang, K. Nishizawa, and C. Fu, 1999: A seasonal cycle simulation over eastern Asia and its sensitivity to radiative transfer and surface processes. *J. Geophys. Res.*, **104**, 6403-6423.

Giorgi, F., and G. T. Bates, 1989: The climatological skill of a regional model over complex terrain. *Mon. Wea. Rev.*, **117**, 2325-2347.

Giorgi, F., M. R. Marinucci, and G. T. Bates, 1993a: Development of a second generation regional climate model (RegCM2) I: Boundary layer and radiative transfer processes. *Mon. Wea. Rev.*, **121**, 2794-2813.

Giorgi, F., M. R. Marinucci, G. De Canio, and G. T. Bates, 1993b: Development of a second generation regional climate model (RegCM2) II: Convective processes and assimilation of lateral boundary conditions. *Mon. Wea. Rev.*, **121**, 2814-2832.

Gong Wei, Li Weiliang, and Zhou Xiuji, 1996: Modeling summer precipitation in China by a modified NCAR RegCM. *Studies on Short-term Climate Variations and Their Formation in China*, H. -X. Cao, Y. -H. Li and F. -Y. Wei, Eds., China Meteorological Press, Beijing, 110-116 (in Chinese).

Grell, G. A., 1993: Prognostic evaluation of assumptions used by cumulus parameterizations. *Mon. Wea. Rev.*, **121**, 764-787.

Holtslag, A. A. M., E. I. F. de Bruijn, and H. L. Pan, 1990: A high resolution air mass transformation model for short-range weather forecasting. *Mon. Wea. Rev.*, **118**, 1561-1575.

Hostetler, S. W., and F. Giorgi, 1992: Use of a regional atmospheric model to simulate lake-atmosphere feedbacks associated with Pleistocene Lakes Lahontan and Bonneville. *Climate Dyn.*, **7**, 39-44.

Leung, L. R., S. J. Ghan, Z. -C. Zhao, Y. Luo, W. -C. Wang, and H. -L. Wei, 1999: Intercomparison of regional climate simulations of the 1991 summer monsoon in eastern Asia. *J. Geophys. Res.*, **104**, 6425-6454.

Liu Yongqiang, R. Avissar, and F. Giorgi, 1996: A simulation with the regional climate model RegCM2 of extremely anomalous precipitation during the 1991 East-Asian flood: An evaluation study. *J. Geophys. Res.* **101**, 26,199–26,215.

Luo Yong, and Zhao Zongci, 1997: Numerical simulation of East Asian regional climate with NCAR RegCM2 *Quarterly Journal of Applied Meteorology*, **8**(Suppl.), 124–133 (in Chinese).

Shea, D. J., K. E. Trenberth, and R. W. Reynolds, 1992: A global monthly sea surface temperature climatology. *J Climate*, **5**, 987–1001.

Trenberth, K. E., and J. G. Olson, 1988: ECMWF Global Analyses 1979–1986: Circulation Statistics and Data Evaluation. NCAR Technical Note, NCAR / TN-300+STR, 94pp.

Wei Helin, Fu Congbin, and W. C. Wang, 1998: The effect of lateral boundary treatment of regional climate model on the East Asian summer monsoon rainfall simulation. *Chinese Journal of Atmospheric Sciences* **22**(3), 231–243.

Wei Helin, and W. C. Wang, 1998: A regional climate model simulation of summer monsoon over East Asia. A case study of 1991 flood in Yangtze-Huaihe Valley. *Advances in Atmospheric Sciences*, **15**(4), 489–509

Wu Xiaoxi, Ding Yihui, and Ma Shufen, 1996: A study of the surface fluxes and structure of mixing layer during the Meiyu heavy rainfall over the Yangtze-Huaihe valley in 1991. *Studies on Meso-Scale Weather and Its Dynamics*, Ding Yihui, Eds., China Meteorological Press, Beijing, 269–281 (in Chinese).

Zhang Jing, 1996: Land surface process model and its coupling with a regional climate model. Ph. D. dissertation, Peking University, 202pp (in Chinese).

Zhao Zongci, and Luo Yong, 1997: Advances in regional climate modeling since 1990. *Acta Meteorologica Sinica*, **11**, 385–406.

NCAR RegCM2 对 1991 年夏季江淮流域异常降水事件中关键物理过程的模拟能力检验

罗 勇 赵宗慈 丁一汇

摘 要

选取 1991 年夏季江淮流域发生的持续性特大暴雨洪涝个例，利用 NCAR 第二代区域气候模式 RegCM2 对逐日降水过程及其关键物理因子进行了数值模拟。模式的侧边界条件由 ECMWF 的大尺度分析资料提供，模拟时间为 1991 年 5–8 月。模式范围包括东亚地区及相邻海域，水平分辨率为 60 km × 60 km，垂直方向为 23 层。试验结果显示，该模式能够合理地模拟出 1991 年夏季东亚地区的逐日降水过程，特别是在江淮流域发生的异常降水事件。对一些关键物理变量和过程时空结构的分析表明，大气垂直速度和水平散度的时间演变与江淮流域的 5 次降水事件一致；形成异常降水的水汽来源主要是大气的水平运动输送。西太平洋副热带高压控制着东亚夏季季风的进退，RegCM2 能够模拟出西太平洋副高的南北位置移动。而且，模式能够较好地再现出对水汽输送至关重要的低空急流的逐日变化。

关键词：区域气候模拟，逐日降水，江淮流域